Functional Analyses of Tyr420 and Leu607 of *Alicyclobacillus acidocaldarius* Squalene-Hopene Cyclase. Neoachillapentaene, a Novel Triterpene with the 1,5,6-Trimethylcyclohexene Moiety Produced through Folding of the Constrained Boat Structure

Tsutomu Sato, Shigehiro Sasahara, Toshiyuki Yamakami, and Tsutomu Hoshino[†]

Department of Applied Biological Chemistry, Faculty of Agriculture, Niigata University, Ikarashi, Niigata 950-2181, Japan

The functions of Tyr420 and Leu607 were analyzed by constructing various site-directed mutants. The mutation at position 420 into Ala and Gly gave bicyclic α- and γ-polypodatetraene in significant amounts, but with a trace amount of tricyclic malabaricatriene. The kinetic data for and the product distribution of the Y420F mutant indicate that the major function of Tyr420 is to stabilize the 6/6-fused bicyclic cation. Mutation experiments on Leu607 demonstrate that the appropriate steric bulk size at position 607 is required to strongly bind with the product-like conformation formed during the polycyclization process. Introduction of the bulkiest Trp residue into 420 or 607 led to the production of a novel monocyclic triterpene having the (5R,6R)-1,5,6-trimethylcyclohexene ring, named neoachillapentaene, indicating that the enzymatic cyclization proceeded *via* a constrained boat structure. Folding of the squalene molecule into a boat conformation by squalene cyclase has not been reported before.

Key words: squalene; hopene; terpene cyclase; unnatural natural product; *Alicyclobacillus acidocaldarius*

The cyclization of squalene **1** into pentacyclic hopene **2** and hopanol **3** is one of the most complicated biochemical reactions (Scheme 1)[1–4] which is catalyzed by squalene-hopene cyclases (SHCs) [EC 5.4.99-] from prokaryotic species. The polycyclization reaction proceeds under precise enzymatic control to form five new rings and nine new chiral centers. This polycyclization mechanism is analogous to that mediated by eukaryotic oxidosqualene cyclases (OSCs) which give lanosterol and numerous plant triterpenes from (3S)-2,3-oxidosqualene.[2–4] In the past several years, there have been remarkable advances with the catalytic mechanism of *Alicyclobacillus acidocaldarius* SHC.[1,2] By using site-directed

mutants and substrate analogs,[1,2] we have established that this polycyclization reaction consists of eight reaction steps (Scheme 1): (1) 1st cyclization to form A-ring **4** by proton attack on the terminal double bond,[5] (2) 2nd ring closure to give the B-ring (6/6-fused A/B ring system **5**),[6] (3) 3rd cyclization to yield the 5-membered C-ring (6/6/5-fused A/B/C-tricyclic ring system **6**) by Markovnikov closure, (4) which then undergoes ring expansion to form the 6-
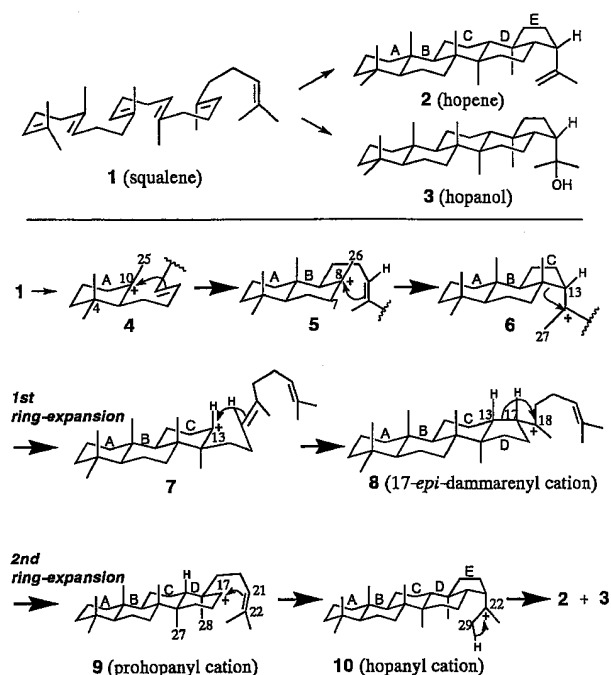
Scheme 1. Polycyclization Reaction of Squalene **1**, Leading to Hopene **2** and Hopanol **3**.

This polycyclization reaction comprises eight reaction steps which has been demonstrated by isolating the abortive cyclization products formed by numerous site-directed mutants and by trapping the carbocation intermediates by using the substrate analogs.[1,2]

membered C-ring (6/6/6-fused tricyclic ring system **7**),[7] (5) 5th cyclization to give the thermodynamically favored 5-membered D-ring (6/6/6/5-fused A/B/C/D ring system **8**, 17-*epi*-dammarenyl cation),[8] (6) followed by the second ring enlargement process to form the 6-membered D-ring (6/6/6/6-fused A/B/C/D-ring system, prohopanyl cation **9**),[9,10] (7) the last ring closure process to construct the 6/6/6/6/5-fused A/B/C/D/E-ring system (**10**, hopanyl cation),[10] and (8) the final deprotonation reaction to introduce the double bond between C-22 and C-29. The polycyclization reaction is characterized by the folding of **1** into an all *pre*-chair conformation during the multiple reaction processes. We have demonstrated that cation-π interaction between π-electrons of aromatic amino acids and the transient carbocations greatly contributed to the acceleration of the polycyclization reaction. The replacement of Phe365,[6] Phe601[7] and Phe605[10] by Tyr greatly enhanced the reaction velocity due to the elevated π-electron density of Tyr. In addition, a few tyrosine residues were shown to intensify the cation-π interaction by being placed at correct positions in the reaction cavity.[11] The steric bulk size of active site residues is likely to be responsible for stereochemical control during the polycyclization reaction; the substitution of Ile with smaller Ala or Gly at position 261 afforded false intermediates having 13α-H in the 6/6/5-fused tricyclic and 17α-H in the 6/6/6/5-fused tetracyclic cation,[9] the configurations of which are opposite to those of true intermediates **6** (13β-H) and **8** (17β-H) (Scheme 1). However, the question has remained unresolved as to how stereochemical specificity is attained along the polycyclization pathway; in other words, why only single stereoisomer **2** is produced, despite stereoisomers of **2**[9] being possible. Matsuda and co-workers have recently reported several examples, in which the steric bulk size of active sites involved in OSCs influenced the polycyclization pathway of oxidosqualene.[12-14] To answer the question about the stereochemical specificity, a number of mutants having different bulk size should be constructed and evaluated.

The two residues of Tyr420 and Leu607 are not highly conserved in all known SHCs. The Tyr420 and Leu607 residues of *A. acidocaldarius* SHC are replaced by Phe and Ile, respectively, in some other bacterial SHCs.[15] However, X-ray information on the SHC-inhibitor complex shows that these residues are located close to the inhibitor of *N*,*N*-dimethyldodecylamine-*N*-oxide (LDAO),[16,17] implying that the two residues may be responsible for catalysis. Indeed, Poralla and co-workers have reported that the Tyr420Ala mutant produced three abortive cyclization products consisting of two bicycles, α- and γ-polypodatetraene, and one tricycle, malabaricatriene,[18,19] and that the Leu607Lys mutant gave bicyclic γ-polypodatetraene.[20] However, no kinetic data were presented. In order to infer the precise catalytic function, numerous mutants have to be constructed, in which Tyr420 and Leu607 are replaced by other differently categorized amino acids with different electronic and/or bulk size environments, and the kinetic data of the mutants have also to be evaluated in detail. We planned to prepare many mutants targeted at positions 420 and 607 in order to provide deeper insight into the functions of Tyr420 and Leu607.

We present here definitive evidence that the major function of Tyr420 is to stabilize bicyclic cation intermediate **5** formed during the polycyclization cascade. Furthermore, we describe that the steric bulk size at position 607 is critical to the optimal folding of **1** leading to **5** having a chair form for the B-ring; the most appropriate bulk size of Leu gives rise to perfect contact around the B-ring formation site. These inferences are drawn from the kinetic data of numerous site-directed mutants targeted at Tyr420 and Leu607 and from the structures of the abortive cyclization products. Replacement by the bulkier amino acids at the two positions, such as Y420→W and L607→F or W, gave an unnatural natural triterpene having the (5*R*,6*R*)-1,5,6-trimethylcyclohexene ring. This carbocyclic triterpene skeleton has never been reported before, despite more than 90 different triterpene skeletons being known at the present time.

Materials and Methods

Analytical method. ^{1}H-NMR and ^{13}C-NMR spectra were measured in a C_6D_6 solution by Bruker DPX 400 and DMX 600 instruments. The chemical shifts of ^{1}H- and ^{13}C-NMR spectra (ppm) are relative to 7.28 and 128.0 ppm for the solvent peak. MS spectra were recorded with a Jeol SX 102 mass spectrometer. GC analyses were carried out by a Shimadzu GC-8A instrument with a DB-1 capillary column (0.53 mm × 30 m; injection temperature, 290°C; column temperature, 270°C; and flow rate of N_2 carrier, 1.0 kg/cm^2). Specific rotation values were measured at 25°C with a Horiba SEPA-300 instrument.

General methods. Details of the experimental protocol have been reported in the previous papers[5,11] for the overexpression systems with the pET vector in *E. coli* BL21 (DE3), DNA sequence analyses, preparation of cell-free homogenates and enzyme purification methods.

Site-directed mutagenesis. All site-directed mutagenesis experiments were performed as described in the previous papers.[5,11] The following primers were used:

Y420G, 5′-pd[CTCGTGTTGTCCACGTC*GCC*GG-CGCCCCAAC]-3′ (−*Sal* I)
Y420A, 5′-pd[GCTCGTGTTGTCCACGTC*GGCG*-

GCGCCCCAACC]-3′ (− *Sal* I)

Y420D, 5′-pd[CTCGTGTTGTCCACGTC*GTC*GG-CGCCCCAAC]-3′ (− *Sal* I)

Y420H, 5′-pd[GTTGTCGACGTC*GTGA*GCGCCC-CAACCG]-3′ (− *Bbe* I)

Y420F, 5′-pd[CTCGTGTTGTCCACGTC*CCA*GG-CGCCCCAAC]-3′ (− *Sal* I)

Y420W, 5′-pd[CTCGTGTTGTCCACGTC*GCC*GG-CGCCCCAAC]-3′ (− *Sal* I)

L607A, 5′-pd[CATGGTGTAGCC*GGC*GTAGAA-ATCCCCGGGGAAGCCCG]-3′ (+ *Sma* I)

L607I, 5′-pd[GGTGTAGCC*GA T*GTAGAAATCC-CCGGGGAAGCCCG]-3′ (+ *Sma* I)

L607F, 5′-pd[CATGGTGTAGCC*GAA*GTAGAA-ATCCCCGGGGAAGCCCG]-3′ (+ *Sma* I)

L607W, 5′-pd[CATGGTGTAGCC*CCA*GTAGAA-ATCCCCGGGGAAGCCCG]-3′ (+ *Sma* I)

The bold letters designate the altered bases, and the italic letters show the target mutations. The underlined letters show the silent mutations for easy screening of the desired mutants by a restriction fragment analysis. The created or deleted restriction sites are shown in parentheses. To ascertain that the desired mutation had been carried out, the entire region of all the inserted DNAs was sequenced.

Thermal stability and kinetic analysis. All the mutated SHCs were homogeneously purified according to the protocol described in the previous paper.[5,11)] A mixed solution, which was composed of 0.5 mM squalene, 0.2% Triton X-100 and 5 μg of the homogeneously purified enzyme in a sodium citrate buffer (60 mM, pH 6.0), was prepared in a final volume of 5 ml for the enzyme reactions. Incubation was done for 60 min at different temperatures (30, 35, 40, 45, 50, 55, 60, 65, or 70°C) to examine the thermal stability of the cyclases. To estimate the kinetic parameters, incubation was conducted for 60 min at 45°C before adding 15% methanolic KOH (6 ml) to terminate the enzyme reaction. The lipophilic products (**2** and **3**) and starting material (**1**) which had remained unchanged were extracted with *n*-hexane (5 ml × 4) from each reaction mixture, and final product **2** was quantified by a GC analysis with a DB-1 capillary column (30 m in length). The kinetic value of K_m and k_{cat} were estimated from Lineweaver-Burk plots.

Isolation and structural determination of products from mutated SHCs. A cell-free homogenates from the cultured *E. coli* cells (6 liters), in which the mutated SHCs of Y420A, Y420W, L607F and L607W were expressed, was prepared as described in the previous papers.[5,11)] Squalene **1** (150 mg, 50 mg, 75 mg and 75 mg, respectively, for Y420A, Y420W, L607F and L607W) was separately incubated with the homogenate at the optimal temperature for 16 h, and the reaction mixture was lyophilized. The product

was extracted with *n*-hexane (200 ml × 3) from each incubated mixture, and then subjected to SiO_2 column chromatography by eluting with *n*-hexane, giving **1**, **2**, **11** and **13–16** in a pure state. A mixed solvent of *n*-hexane and EtOAc (100:2) was used to elute **3** and **12** due to the high polarity. The complete purification of **12** was achieved by HPLC [*n*-hexane:isopropanol = 100:0.1]. The following yields were obtained: **1** (3.6 mg), **2** (94.3 mg), **3** (11.3 mg), **14** (9.1 mg), **15** (21.2 mg) and **16** (1.4 mg) for Y420A; **1** (3.5 mg), **2** (0.3 mg), **11** (3.2 mg), **13** (26.7 mg), **14** (6.0 mg) and **15** (3.3 mg) for Y420W; **1** (12.5 mg), **2** (0.6 mg), **11** (4.3 mg), **12** (0.5 mg), **13** (39.1 mg), **14** (6.8 mg) and **15** (4.9 mg) for L607F; and **1** (0.5 mg), **11** (7.3 mg), **12** (0.4 mg), **13** (53.7 mg) and **14** (8.0 mg) for L607W.

The structures of **11–16** were determined by spectral analyses with EIMS and NMR, including COSY 45, HOHAHA, NOESY, DEPT, HMQC and HMBC. Products **13**, **14** and **16** were 3-deoxyachilleol, γ-polypodatetraene and 17(*E*)-13α(*H*)-malabarica-14(27),17(*E*),21-triene, respectively, the complete NMR assignments of which have been reported before.[6,7,11)] The spectroscopic data (NMR assignment, EI-MS and specific rotation) for **11**, **12** and **15**, which had not previously been isolated in our experiments, are described below.

Compound **11** (oil, neoachilla-3,9(*E*),13(*E*),17(*E*), 21-pentaene (*cf* IUPAC name: 1,5(*R*),6(*R*)-trimethyl-6-[3,8,12,16-tetramethyl-heptadeca-3(*E*), 7(*E*),11(*E*),15(*E*)-tetraenyl]-cyclohexene). The ^{1}H- and ^{13}C-NMR data measured at 400 MHz are shown in Table 1. EIMS fragments m/z (%): 410 (16) [M^+], 395 (1) [M^+ − Me], 341 (9), 273 (1), 205 (12), 137 (26), 123 (100) [trimethylcyclohexene ring], 69 (63). HREIMS for $C_{30}H_{50}$: calcd., 410.3913; found, 410.3888. $[\alpha]_D^{25}$ − 4.6 (c = 0.27, $CHCl_3$).

Compound **12** (oil, 6α-hydroxyachilla-9(*E*), 13(*E*),17(*E*),21-tetraene). 600 MHz, δ_H (ppm): 5.53 (1H, bt, J = 6.4 Hz, H-10), 5.46 (1H, bt, J = 6.1 Hz, H-13), 5.42 (1H, t, J = 6.1 Hz, H-17), 5.37 (1H, t, J = 7.0 Hz, H-21), 2.48 (1H, m, H-8), 2.32 (4H, m, H-16 and H-20), 2.31 (5H, m, H-8, H-11 and H-12), 2.22 (4H, m, H-15 and H-19), 1.84 (3H, s, H-26), 1.83 (1H, m, H-7), 1.80 (3H, s, H-29), 1.75 (3H, s, H-28 or H-27), 1.74 (3H, s, H-27 or H-28), 1.72 (1H, m, H-1), 1.69 (3H, s, H-30), 1.56 (1H, m, H-7), 1.50 (1H, m, H-2), 1.41 (1H, m, H-2), 1.35 (1H, m, H-3), 1.29 (1H, ddd, J = 3.7, 12.6, 12.6 Hz, H-1), 1.20 (1H, ddd, J = 4.2, 12.7, 12.7 Hz, H-3), 1.20 (3H, s, H-25), 1.15 (1H, t, J = 4.5 Hz, H-5), 1.05 (3H, s, H-23), 0.87 (3H, s, H-24). δ_C (ppm): 136.5 (C-9), 135.21 (C-14), 134.94 (C-18), 131.07 (C-22), 124.95 (C-21), 124.88 (C-17 or C-13), 124.84 (C-13 or C-17), 124.7 (C-10), 73.5 (C-6), 56.85 (C-5), 43.95 (C-1), 43.39 (C-8), 41.76 (C-3), 40.22 (C-15 or C-19), 40.19 (C-19 or C-15), 35.59 (C-4), 32.93 (C-23), 28.78 (C-11 or C-12), 28.75 (C-11 or C-12), 27.22 (C-16 or C-20),

27.13 (C-20 or C-16), 25.81 (C-29), 25.34 (C-7), 23.5 (C-25), 21.59 (C-24), 20.84 (C-2), 17.71 (C-30), 16.33 (C-26), 16.19 (C-28 or C-27), 16.09 (C-27 or C-28). The relative stereochemistry was confirmed by the NOE cross peak of Me-23 with H-5 and that of Me-24 with Me-25. EIMS fragments m/z (%): 428 (0.7) [M$^+$], 410 (21) [M$^+$ − H$_2$O], 395 (3) [M$^+$ − H$_2$O − Me], 341 (8), 273 (3), 205 (30), 137 (73) [allylic cleavage between C-7 and C-8], 69 (100). HREIMS for C$_{30}$H$_{50}$ M$^+$ − H$_2$O): found, 410.3905. $[\alpha]_D^{25}$ +0.5 (c 0.0034, CHCl$_3$), cf $[\alpha]_D^{23}$ +2.5 (c 0.6, CHCl$_3$).[21]

Compound **15** (oil, α-polypodatetraene). 600 MHz, δ_H (ppm): 5.46 (1H, bt, J = 7.1 Hz, H-13), 5.44 (1H, bt, J = 7 Hz, H-17), 5.37 (1H, bt, J = 6.9 Hz, H-21), 5.09 (1H, bs, H-26), 4.84 (1H, bs, H-26), 2.51 (1H, ddd, J = 12.8, 4.7, 2.4 Hz, H-7), 2.43 (1H, m, H-12), ~2.3 (4H, m, H-15, H-16, H-19 and H-20), 2.16 (1H, m, H-12), 2.10 (1H, ddd, J = 12.8, 12.8, 4.7 Hz, H-7), 1.82 (1H, m, H-1), 1.81 (3H, s, H-29), 1.78 (1H, m, H-9), 1.77 (3H, s, H-27), 1.75 (1H, m, H-6), 1.74 (3H, s, H-28), 1.69 (3H, s, H-30), 1.69 (1H, m, H-11), 1.64 (1H, m, H-2), 1.62 (1H, m, H-11), 1.55 (1H, m, H-2), 1.48 (1H, bd, J = 12.9 Hz, H-3), 1.42 (1H, dddd, J = 12.9, 12.9, 12.9, 4.2 Hz, H-6), 1.27 (1H, ddd, J = 12.9, 12.9, 3.8 Hz, H-3), 1.12 (1H, dd, J = 12.6, 2.5 Hz, H-5), 1.08 (1H, ddd, J = 13.0, 13.0, 3.6 Hz, H-1), 0.967 (3H, s, H-23), 0.921 (3H, s, H-24), 0.865 (3H, s, H-25). δ_C (ppm): 148.85 (C-8), 135.0 (C-14), 134.97 (C-18), 131.08 (C-22), 125.73 (C-13), 124.94 (C-21), 124.84 (C-17), 106.65 (C-26), 56.46 (C-9), 55.66 (C-5), 42.43 (C-3), 40.24 (C-15 or C-19), 40.23 (C-15 or C-19), 39.82 (C-10), 39.31 (C-1), 38.73 (C-7), 33.71 (C-4), 33.65 (C-23), 27.38 (C-12, C-16 or C-20), 27.25 (C-12, C-16 or C-20), 27.15 (C-12, C-16 or C-20), 25.82 (C-29), 24.77 (C-6), 24.23 (C-11), 21.89 (C-24), 19.75 (C-2), 17.72 (C-30), 16.17 (C-28), 16.12 (C-27), 15.61 (C-25). The relative stereochemistry was confirmed by the NOE cross peaks among H-5, H-9 and Me-23. EIMS fragments m/z (%): 410 (26) [M$^+$], 395 (18) [M$^+$ − CH$_3$], 341 (3), 273 (8), 205 (7), 204 (4), 191 (12) [allylic cleavage between C9 and C11], 137 (51), and 69 (100). HREIMS for C$_{30}$H$_{50}$: found, 410.3921. $[\alpha]_D^{25}$ +14.2 (c 0.046, CHCl$_3$), cf +27.4 (c 0.4, CHCl$_3$).[22]

Product distribution pattern. One mg of **1** was separately incubated at 45°C for 16 h with cell-free extracts from the mutants of Y420G, Y420D, Y420H, Y420F, and L607A and L607I (Table 3), which had been grown in a 50-ml LB medium. The hexane extract was obtained from the reaction mixture. The detergent was removed by passing through a short SiO$_2$ column [*n*-hexane:EtOAc = 100:20], before the extract was subjected to a GC analysis to examine the product distribution pattern and the product amount. The enzymatic products were identified by comparing the GC-MS fragment patterns with those of authentic samples, which had previously been isolated by us, and quantified by a GC analysis.

Results

To provide insight into the functions of Tyr420 and Leu607, the following ten mutants were constructed: Y420G, Y420A, Y420D, Y420H, Y420F, Y420W, L607A, L607I, L607F and L607W. Tyr is an aromatic amino acid having a phenolic hydroxyl group. To examine the role of the hydroxyl group and the aromatic π-electron system of the Tyr residue, the Tyr was mutated into Phe and Trp. To diminish the role of the aromatic π-electrons, the Y420G and Y420A mutants were prepared. The mutation experiments for the Tyr into Asp and His were carried out to evaluate how the acidic function of Asp (or anion of the carboxylate) and the π-electron density of His (or the basic function of proton-abstraction) would affect the polycyclization cascade. To get better knowledge about the steric bulk size at position 607, Ala with a smaller bulk size and Ile with an equivalent size were introduced. The Phe and Trp mutants were also constructed to evaluate the effect of the aromatic ring on the polycyclization reaction.

Enzymic products formed by the site-directed mutants

We have previously shown that point mutants, altered at active sites, afforded prematurely cyclized products. Based upon the product distribution, the placement of various active residues inside the central active cavity has been proposed.[1,2] With a large amount of the cell-free homogenate from the grown mutants, **1** was incubated for 16 h at the optimal temperature and the enzymic products formed by each mutant were analyzed by GC. As one example, the product distribution pattern by the L607F mutant is shown in Fig. 1. Five abortive cyclization compounds (**11–15**) were produced by the L607F mutant (Figs. 1 and 2). All the enzymic products were purified by SiO$_2$ column chromatography, and their structures determined by detailed NMR analyses including 2D NMR (COSY 45, HOHAHA, NOESY, HMQC and HMBC), these beeing confirmed by the EI-MS fragment patterns. Products **13** and **14** were 3-deoxyachilleol and γ-polypodatetraene, respectively, which had previously been isolated by us.[5,6] Product **15** was confirmed to be α-polypodatetraene by the detailed NMR analyses (see the Materials and Methods section). The production of **11** and **12** has not been reported before. The structural determination of **11** and **12** is described later. Prolonged incubation with the Y420G and Y420A mutants afforded three products: bicyclic **14** and **15** and tricyclic **16**. Compound **16** was determined to be (17*E*)-13α(*H*)-malabarica-14(27),17,21-triene by the NMR and EI-
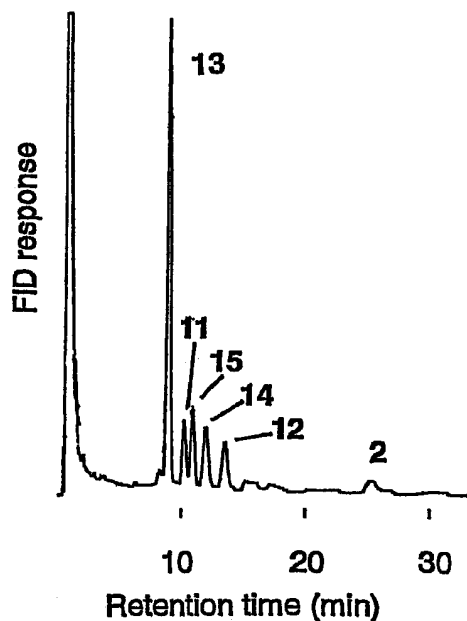
Fig. 1. Product Distribution Pattern of the Leu607Phe Mutant by a GC Analysis.

Five abortive cyclization products (**11–15**) having mono- or bicyclic skeletons were found in addition to **2**. One mg of **1** was incubated with a cell-free extract in a 200-ml culture under catalytically optimal conditions (55°C and pH 6.0), whereby all employed **1** was consumed. Triton X-100 was removed by passing the hexane extract of the reaction mixture through a short SiO_2 column with a mixture of hexane: EtOAc (100:20) as the eluent (see the Materials and Methods section). The amount of the mutated SHC used, equivalent to 2 mg of pure Leu607Phe SHC, was significantly larger than that in Fig. 4 and Table 3 by 400-fold and 4-fold, respectively.
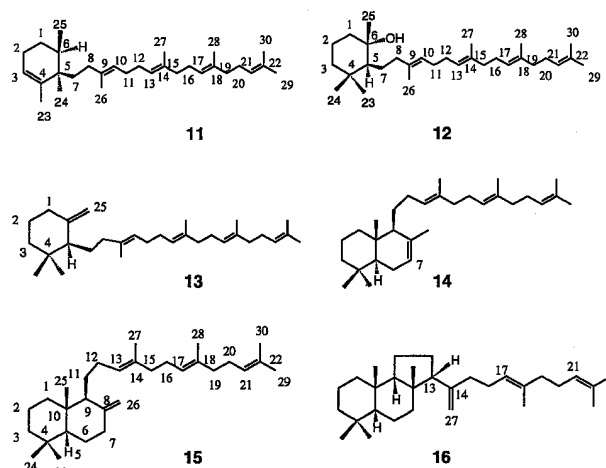

Fig. 2. Structures of the Abortive Cyclization Products Isolated by Some Mutated SHCs Constructed in This Paper.

We propose neoachillapentaene as the name for unnatural natural triterpene **11**. Products **12**, **13**, **14**, **15** and **16** were known 6-α-hydroxy-9(*E*),13(*E*),17(*E*),21-tetraene, 3-deoxyachilleol, γ-polypodatetraene, α-polypodatetraene, and 17(*E*)-13α(*H*)-malabarica-14(27),17,21-triene, respectively.

MS analyses, and had previously been isolated from mutants F601A and I261A.[7,9] All the abortive cyclization products discussed in this paper are listed in Fig. 2. The abortive cyclization products were not found in any detectable amount when the kinetic data were estimated by incubating **1** with small amounts of the SHCs (5 μg) and for a short incubation time (60 min) (see Table 2 and Fig. 4), but were detected when using large amounts of the SHCs and by incubating for a prolonged period of incubation time (16–20 h) (see Table 3 and Fig. 1).

Structural determination of 11

Substrate **1** had eight allyl methyl groups and six double bonds in the molecule. In the ¹H-NMR spectrum of **11**, six allyl methyl protons were found at δ_H 1.80, 1.79, 1.77, 1.740, 1.736 and 1.69, suggesting that four double bonds remained unchanged without participating in the cyclization reaction, inferring that **11** was a monocyclic compound. The other two methyl protons appeared in a higher field of δ_H 0.98 (d, *J* = 6.8 Hz, Me-25) and δ_H 1.01 (s, Me-24), suggesting that the secondary and tertiary methyl groups was on the cyclized monocyclic ring. The clear HMBC cross peaks of the two methyl protons of δ_H
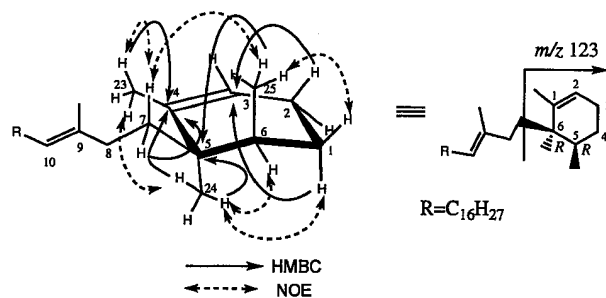

Fig. 3. Selected HMBC, NOEs and EI-MS Fragment Ion (*m/z* 123, base peak) Data for the Structural Determination of **11**.

No NOE was found between Me-24 and Me-25, or between H-6 and H-7. The numbering on the left side is according to the neoachillapentaene skeleton, while that of the 1,5,6-trimethylcyclohexene ring (the right side) is to IUPAC nomenclature.

1.01 (Me-24) and δ_H 1.79 (bs, Me-23) with δ_C 139.7 (s, C-4) indicate that one allyl methyl group (Me-23) and one tertiary methyl group (Me-24) were attached to the monocyclic ring having a double bond (Fig. 3). In addition, the protons of both Me-25 and Me-24 were correlated with C-5 (s, δ_C 40.7) in the HMBC spectrum, confirming the position of Me-25. The double bond position was further confirmed by the HMBC cross peaks of both δ_H 1.52 (H-1) and δ_H 2.03 (H-2) with δ_C 124.5 (d, C-3). These data definitively demonstrate the presence of the 1,5,6-trimethylcyclohexene moiety in **11** (IUPAC numbering). The trimethylcyclohexene ring was further supported by observing *m/z* 123 as a base peak in the EI-MS spectrum (Fig. 3). The relative stereochemistry of the 1,5,6-trimethylcyclohexene ring was determined by the NOESY spectrum. Strong NOEs of Me-24 with H-6 and of Me-25 with H-7 revealed the same geo-

Table 1. ^{1}H- and ^{13}C-NMR Data for Compound **11** (neoachillapentaene) in C_6D_6
The position numbering is according to Fig. 2.

Position	^{1}H	^{13}C	Position	^{1}H	^{13}C
1	1.52 (1H, m); 1.59 (1H, m)	27.4 (t)	16	2.32 (2H, m)	27.1 (t)[b]
2	2.03 (1H, m); 2.09 (1H, m)	25.9 (t)	17	5.46 (1H, m)[a]	124.8 (d)
3	5.56 (1H, bm)	124.5 (d)	18	—	134.9 (s)
4	—	139.7 (s)	19	2.23 (2H, m)	40.2 (t)
5	—	40.7 (s)	20	2.32 (2H, m)	27.2 (t)[b]
6	1.88 (1H, m)	33.5 (d)	21	5.37 (1H, bt, J = 6.8 Hz)	124.9 (d)
7	1.70 (1H, m); 1.67 (1H, m)	35.6 (t)	22	—	131.1 (s)
8	1.93 (1H, m); 2.14 (1H, m)	34.7 (t)	23	1.79 (3H, bs)	19.4 (q)
9	—	136.2 (s)	24	1.01 (3H, s)	21.2 (q)
10	5.46 (1H, m)	124.2 (d)	25	0.98 (3H, d, J = 6.8 Hz)	16.0 (q)
11	2.28 (2H, m)	28.7 (t)	26	1.77 (3H, s)	16.4 (q)
12	2.28 (2H, m)	28.7 (t)	27	1.74 (3H, s)[c]	16.2 (q)[c]
13	5.42 (1H, bt, J = 7.0 Hz)[a]	124.8 (d)	28	1.736 (3H, s)[c]	16.1 (q)[c]
14	—	135.2 (s)	29	1.80 (3H, s)	25.8 (q)
15	2.23 (2H, m)	40.2 (t)	30	1.69 (3H, s)	17.7 (q)

[a,b,c] The assignments may be interchangeable.

metry between Me-24 and H-6, and between Me-25 and H-7, but no NOE was observed between Me-24 and Me-25, or between H-6 and H-7. The selected NOE data are shown in Fig. 3. Thus, the relative stereochemistry of the 5- and 6-positions in the 1,5,6-trimethylcyclohexene ring was determined to be all R-configuration. The results of the detailed NMR analyses are consistent with the proposed structure for **11** shown in Fig. 2. The complete NMR assignments are shown in Table 1. Compound **11** is a novel triterpene, which we name neoachillapentaene for unnatural natural product **11**.

Structural determination of 12

Compound **12** had high polarity, i.e., no movement on SiO_2 TLC, but other products **11** and **13–16** showed R_f values in the range 0.45–0.75 for hexane. The observation of the fragment ion $M^+ - H_2O$ (m/z 410) also suggested the involvement of a hydroxyl group in **12**, which was confirmed by finding the signal at δ_C 73.5 (s, C-6), a diagnostic signal for an alcoholic carbon, in the ^{13}C-NMR spectrum. Five allyl methyl groups and four double bonds were left unchanged without any responsibility for the cyclization reaction, indicating the monocyclic ring for **12**. The position of the hydroxyl group was confirmed by the HMBC cross peak of Me-25 with C-6. The relative stereochemistry was determined from the NOESY spectrum: clear NOEs of Me-24 and Me-25, and of Me-23 with H-5, indicating a chair structure for the monocyclic ring. All the NMR data support **12** being 6α-hydroxyachilla-9(E),13(E),17(E),21-tetraene, which has previously been isolated from the fern, *Polypodiodes formosana*.[21]

Functional analysis of Tyr420

Figure 4 shows the specific enzyme activities for the formation of **2** plotted against the incubation temper-

ature by using the homogeneously purified enzymes. The Phe mutant had an optimal temperature of 65°C, higher than that of the native SHC (Fig. 4A), suggesting that reinforcement of the protein structure had acted against thermal denaturation. However, the specific enzyme activity was relatively less than that of the wild-type, strongly indicating that the Tyr residue of the wild-type had acted to stabilize the transient carbocation intermediate. Table 2 shows the kinetic data, which were estimated from the amount of **2** produced. Despite the Phe mutant having enhanced affinity to **1** (the smaller K_m by 1.75-fold), the reaction velocity (k_{cat}) was significantly decreased by 3.6-fold, in a comparison with the wild-type. This finding unequivocally indicates that the free electron pair of the phenolic hydroxyl group played a crucial function for stabilizing the transient cationic intermediate produced during the polycyclization reaction. However, the Trp mutant showed little activity, despite an enhanced cyclization rate being expected owing to the increased π-electron density. This loss of the enzyme activity would be attributable to the significantly decreased binding with **1**, which resulted from the increased steric bulk size. We have previously indicated that an appropriate bulk size is required for effective cation-π interaction; the F365Y mutant had a greater reaction velocity than the F365W mutants.[6] The His mutant had higher activity, when compared to the Ala and the Asp mutants (Table 2). This may provide additional evidence for the crucial role of aromatic π-electrons at position 420, since His moiety not only abstracts a proton as a base, but also stabilizes the transient intermediate through cation-π interaction.

As already described, prolonged incubation with a large amount of Y420G- and Y420A-mutated SHC afforded two bicycles (**14** and **15**) and one tricycle (**16**) as abortive cyclization products, as shown in Table 3.

Table 2. Kinetic Data and Optimal Temperatures for the Wild-type and Mutated SHCs

The kinetic values of K_m and k_{cat} were determined from Lineweaver-Burk plots by using 5 μg each of the homogeneously purified SHCs. The enzyme activities were assayed by estimating the amount of **2** produced after incubating after 45°C for 60 min, where no thermal denaturation occurred. In the cases of the three mutants of Y420W, L607F and L607W, the production of all the enzymic products (**2**, **3** and abortive cyclization products **11–16**) was too small to estimate the kinetic parameters.

SHC	K_m (μM)	k_{cat} (min^{-1})	k_{cat}/K_m	Relative activity (%)	Optimal temperature (°C)
Wild-type	1.62×10	51.8	3.19	100.0	60
Y420G	2.56×10^2	1.21	4.73×10^{-3}	0.1	50
Y420A	9.09×10	13.2	1.45×10^{-1}	4.5	55
Y420D	8.22×10	15.1	1.83×10^{-1}	5.7	55
Y420H	6.89×10	46.6	6.76×10^{-1}	21.2	50
Y420F	0.926×10	14.4	1.56	48.8	65
Y420W	ND	ND	ND	ND	55
L607A	8.78×10	57.8	6.58×10^{-1}	20.6	55
L607I	11.5×10	59.9	5.21×10^{-1}	16.3	55
L607F	ND	ND	ND	ND	55
L607W	ND	ND	ND	ND	55

ND: No enzymic product including the abortive cyclization products (**11–16**) was found.
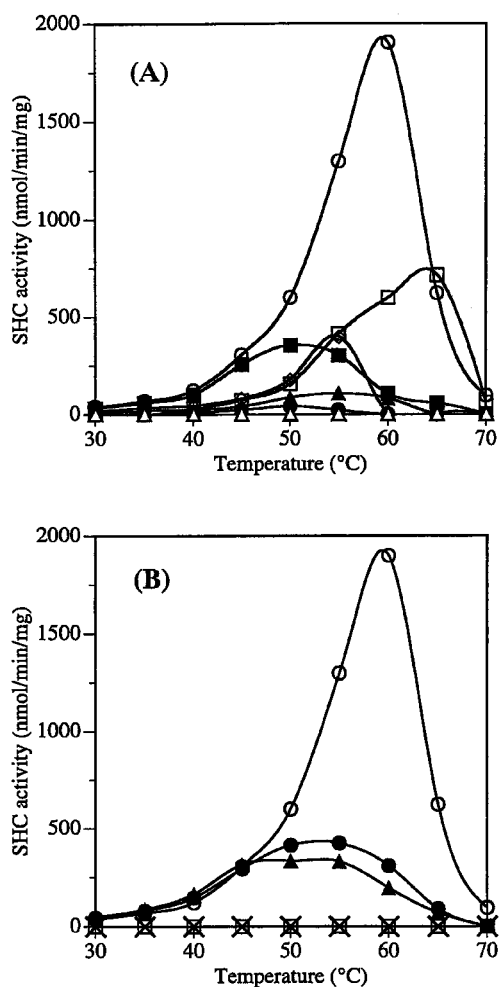
Fig. 4. Specific Enzyme Activities of the Mutated and Wild-type SHCs Plotted against the Incubation Temperatures, These Being Estimated from the Production of Hopene **2**.

One mg of **1** was incubated with 5 μg of a homogeneously purified SHC for 60 min at pH 6.0.

(A) Mutated SHCs targeted at Y420: ○ wild-type, ● Y420G, ▲ Y420A, ◇ Y420D, ■ Y420H, □ Y420F, △ Y420W (B) Mutated SHCs targeted at L607: ○ wild-type, ● L607A, ▲ L607I, □ L607F, × L607W

The Y420F and Y420D mutants afforded only bicyclic **14** and **15**. The Y420H gave mono-**13**, and bicyclic **14** and **15**. It is noteworthy that the Trp mutant gave significant amounts of monocyclic **11** and **13**, together with relatively small amounts of bicycles **14** and **15** and a trace of **2**. Except for the Trp mutant, all the mutants afforded a significant amount of **2**. The ratio of the product distribution is summarized in Table 3. All the mutants other than the Trp mutant produced large amounts of bicyclic compounds, indicating that Tyr420 was situated close to the C-8 cation of **5** during the polycyclization reaction and thus could stabilize cationic intermediate **5** through the phenolic hydroxyl group. The significantly bulky Trp residue, which was incorporated in the mutated SHC, may have interfered with the 2nd cyclization reaction, thus resulting in a high production ratio of monocyclic **13** to bicyclic **14** and **15**.

Functional analysis of Leu607

As shown in Fig. 4B, the mutations of Leu into Ala and Ile dramatically decreased the specific activity for the production of **2**. This could be explained in terms of the increased K_m values, but not of the decreased k_{cat} values (Table 2); that is, the bindings with **1** were dramatically decreased, but the cyclization velocities were nearly the same. The Ala mutant had significantly lower binding to **1** by 5.4 fold, indicating that the enzyme perturbation had occurred, possibly due to the markedly lower bulk size of Ala. However, it is surprising that the mutation of Leu into Ile gave rise to a markedly increased K_m value by 7.1 fold, despite the steric bulk size of Ile being almost equivalent to that of Leu. The structural difference is just a branching point: *iso*-butyl for Leu and *sec*-butyl for Ile. The remarkable difference in K_m value between the Leu and the Ile mutants strongly indicates that the isobutyl residue of Leu 607 more precisely fitted to the folded product-like conformation of **1**, when

Table 3. Product Distribution (%) of the Wild-type and Mutated SHCs Estimated by GC Analyses

One mg of **1** was incubated with a large amount of the cell-free homogenate from 50 ml of cultured cells, equivalent to 0.5 mg of each pure SHCs, under the conditions of pH 6.0, 45 °C and 16 h. Under these conditions, the conversion ratio of **1** to all the enzymic products (**2**, **3** and abortive cyclization products **11–16**), was as follows: 95.3% for Y420G, 17.5% for Y420W, 26.5% for L607F, 20.8% for L607W and 100% for the other mutants, while the wild-type SHC consumed all of **1** in a short incubation time of 60 min. The small conversion ratios of Y420W, L607F and L607W indicate that the activity for the formation of all the enzyme products was decreased and that some of **1** was left unchanged.

| SHC | Hopene | Hopanol | Monocyclic | | | Bicyclic | | Tricyclic | Total yield of |
	2	**3**	**11**	**12**	**13**	**14**	**15**	**16**	**11–16**
Wild-type	84.1	15.9	—	—	—	—	—	—	—
Y420G	47.9	9.3	—	—	—	11.3	28.1	3.4	42.8
Y420A	62.7	11.7	—	—	—	6.9	16.8	1.9	25.6
Y420D	63.4	12.3	—	—	—	7.6	16.7	—	24.3
Y420H	63.7	12.1	—	—	9.1	1.5	13.6	—	24.2
Y420F	75.1	15.0	—	—	—	0.9	9.0	—	9.9
Y420W	0.4	—	9.6	—	69.9	12.2	4.9	—	99.6
L607A	84.8	15.2	—	—	—	—	—	—	—
L607I	84.1	14.3	—	1.6	—	—	—	—	1.6
L607F	1.6	—	9.0	4.8	45.3	21.1	17.9	—	98.1
L607W	—	—	10.1	4.9	74.6	10.4	—	—	100

compared to the *sec*-butyl group of Ile. The enzyme activities of the L607F and L607W mutants for the formation of **2** were almost quenched (Fig. 4B and Table 2), suggesting that this position could not work to stabilize the intermediary carbocation through cation-π interaction. The significantly decreased specific activity, *i.e.* the initial velocity (Fig. 4 and Table 2) should be explained in terms of the bulkiness of Phe and Trp. The bulky substituents may have disturbed the access of **1** to the protonation site (the DXDDTA motif[5]) which is responsible for initiating the polycyclization reaction. However, the prolonged incubation of the L607F and L607W mutants afforded significant amounts of mono- and bicyclic compounds **11–15** without completing the polycyclization to final product **2** (Table 3). No tricyclic product such as **16** was found. This distribution pattern for the abortive cyclization products suggests that L607 was located around the B-ring formation site. The L607F mutant gave significant amounts of bicyclic products **14** and **15**, but the L607W mutant afforded monocyclic **11–13** in larger amounts than the L607F mutant did. This observation indicates that the larger the steric bulk size, the higher the production of monocyclic compounds. Therefore, Leu607 may possibly be positioned around the B-ring formation site, the bulk size at this position being critical to the optimal folding of **1** leading to **5**. A comparison of the product distribution pattern of the Tyr420 mutants with that of the Leu607 mutants suggests that the location sites of the two residues in the interior cavity were close to each other. The position of Leu607 may possibly be closer to the A-ring formation site compared to that of Tyr420, because the L607W mutant gave higher production of monocycles than the Y420 W mutant (Table 3).

Discussion

The formation mechanisms for products **12–16** are explained as follows. Monocyclic **12** and **13** could have been formed from monocyclic cation **4**; deprotonation at the 25-position gave **13**, while **12** was produced as a result of nucleophilic attack of water molecule to the cation **4**. Deprotonation reactions at the 7- and 26-positions of bicyclic intermediate **5** afforded **14** and **15**, respectively. Compound **16** could have been produced by the deprotonation of Me-27 from the 6/6/5-fused tricyclic cation, whose stereochemistry at C-13 was opposite to that of true intermediate **6**.

The kinetic results for the Tyr420 mutants (Table 2) clearly indicate that the function was to stabilize the transient carbocation formed during the polycyclization reaction. Figure 4(A) and Table 2 show that the higher the electron density, the faster the reaction rates. The π-electron density of Tyr (the wild type) is higher than that of Phe (the Y420F mutant), while the steric bulk size of Tyr (the wild-type) is somewhat larger than that of Phe (the Phe mutant), leading to enzyme perturbation. This may have caused the higher thermal stability of the wild-type (Fig. 4 and Table 2); the optimal temperature for the wild-type having the Tyr residue (60 °C) was lower than that for the Phe mutant (65 °C). This inference is consistent with our previous report that the replacement of F365 and F605 by Tyr enhanced the reaction velocity, but the optimal temperatures was decreased.[6,10] It is thus evident that the function of Tyr420 was for stabilizing the cationic intermediate. The decreased electron density of the Phe mutant, compared to that of the wild-type (Tyr residue), could afford bicyclic **14** and **15**, in spite of the in-

A

17 (striatene)   **18** (striatol)

19 (agelasidine B)

       20   **17–19**

B

21
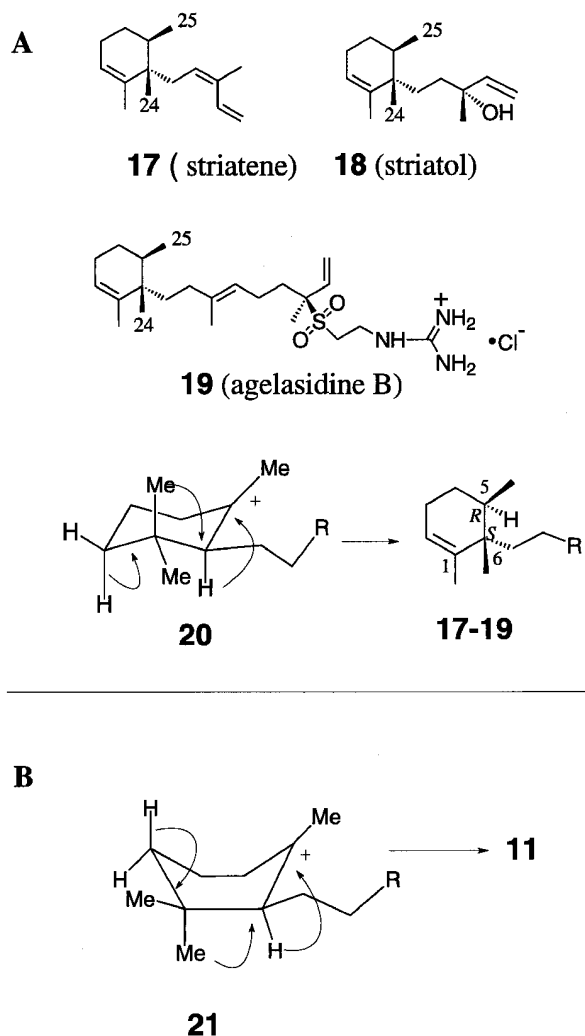
Fig. 5. (A) Natural Sesqui- and Diterpenes Containing 1,5,6-Trimethylcyclohexene Ring.

A chair conformation was adopted for the A-ring formation to yield the stereochemistry of 5*R*,6*S* in the ring of **17–19**. The hydride, methyl shifts and proton elimination reactions proceeded in an anti-parallel concerted manner. (B) Boat Form to Give the Stereochemistry of 5*R*,6*R* in the Cyclohexene Ring of **11**.

creased binding to **1** (Table 2). In addition, the loss of π-electrons by introducing an aliphatic amino acid halted the polycyclization at the bicyclic ring stage, leading to the high production of **14** and **15** (Table 3). These findings strongly indicated that the Tyr420 residue was oriented near the C-8 cation of **5** in the reaction cavity. We have previously shown that residues Phe365[6] and Tyr609[11] also worked to stabilize the C-8 cation in **5**. The amounts of bicyclic compounds produced by the F365A, Y609A and Y420A mutants were *ca.* 96%, 50% and 24%, respectively, indicating that stabilization of the C-8 cation may have been attained mainly by the π-electrons of Phe365, but further enhanced by those of Tyr609 and Tyr420. The results of the X-ray analysis show that the faces of the expanded π-electron system of the F365, F601 and F605 residues were in the direction of

the LDAO inhibitor, thus the planar skeleton of the three Phe residues could stabilize the cationic intermediates through a cation-π interaction.[6,7,10] On the other hand, the hydroxyl group of the Tyr420 residue was arranged to point toward the inhibitor inside the interior cavity.[16,17] The unshared electron pair of the hydroxyl group, whose electron density was further enhanced by the extended resonance through the phenyl π-electron ring system, may have been placed in the proximity to the C-8 cation of **5**, thus resulting in greatly enhanced stabilization of **5**. Alternatively, the negative charge of the phenolate of Tyr420 may have worked for cation stabilization. It was recently reported that a variety of the abortive cyclization products, including bicyclic **14** and **15**, tetra- and pentacyclic skeletons, are accumulated in nearly equivalent amounts in *Zymomonas mobilis* cells.[23] *Z. mobilis* SHC has Phe residue at the position corresponding to Tyr420 of *A. acidocaldarius* SHC.[15] The formation of bicyclic **14** and **15** by *Z. mobilis* SHC may possibly be attributable to the poorer electron density of Phe than of Tyr, as demonstrated here (Tables 2 and 3). The production of energetically unfavorable product **15** was higher than that of favorable **14** (a deprotonation product according to Zaitsev's rule), possibly suggesting that a basic amino acid for abstracting a proton from Me-26 of **5** may have been located near the Tyr420 residue. The Gly and the Ala mutants having smaller bulk size afforded tricyclic **16** (a Markovnikov adduct). The stereochemistry of 13α-*H* is opposite to that of a true 6/6/5-fused tricyclic intermediate (13β-*H*) **6** (see Scheme 1),[7,9] suggesting that erroneous folding of **1** may have occurred during the polycyclization process. The significantly altered enzyme structure, which was verified by the markedly increased K_m values (15.8-fold for the Gly mutant and 5.6-fold for the Ala mutant), may have led to this erroneous folding. This finding may suggest that an appropriate steric bulk size is required at this position to complete the normal polycyclization. However, this function is minimal, because production of **16** is too low to allocate the role of stereochemical control to this position (only 2–3% of all the enzymic products, Table 3). The Y420H mutant gave monocyclic **13**, having an exocyclic methylene group, suggesting that the His residue could also have had a basic function responsible for proton elimination from Me-25 of **4**, in addition to the cation-stabilizing function (a close k_{cat} value to that of the wild-type, Table 2).

Of particular interest is the fact that the Y420W and L607W mutants both produced a novel product **11** having the 1,5,6-trimethylcyclohexene ring. The CD spectra of the mutants were indistinguishable from that of the wild-type (data not shown), suggesting that there was little alteration of the protein structure by the mutations. A few sesqui- and diterpenes having the trimethylcyclohexene ring have been

found in the liverwort, *Ptychanthus striatus*[24] and in the Okinawan sea sponge (Fig. 5).[25] However, the stereochemistry at the 6-position of the trimethylcyclohexene ring (IUPAC numbering) in **11** is opposite to that of striatene **17** and striatol **18** (sesquiterpenes) and agelasidine B **19** (diterpene). Compounds **17–19** could be produced *via* an organized chair structure **20**, which underwent the sequential 1, 2-shift reactions of hydride and methyl group with subsequent deprotonation (Fig. 4(A)), in anti-parallel concerted manner. On the other hand, **11** could have been formed *via* boat structure of **21** as shown in Fig. 5(B), taking into consideration the stereochemistry (5*R*,6*R*) of the trimethylcyclohexene ring (IUPAC numbering). We have most recently reported that a constrained boat form was also constructed from the cyclization of the 10-ethylated-2, 3-oxidosqualene by lanosterol synthase, leading to the monocyclic triterpene having the 2,3,4-trimethylcyclohexanone ring;[26] the bulky ethyl group enforced a boat conformation upon the substrate analog, once cyclization had started in the enzyme cavity. The large steric bulk size of the Trp residue of the Y420W and L607W mutants would have significantly interfered with the access of **1** to the protonation site (the DXDDTA motif[5]), resulting in a remarkably decreased initial velocity (Fig. 4 and Table 2). However, once cyclization had started during the prolonged incubation, **1** would have been constrained to fold with a boat structure **21**; the large bulk size of the replaced Trp residue would have disturbed the formation of the normal chair conformation. This notion is in good agreement with the fact that the bulky ethyl group (increment of the C1 unit to **1**) at the 10-position imposed a boat structure to give the trimethylcyclohexanone ring. However, the Trp mutant could still have adopted a chair form for the A-ring formation (**12** and **13**); the amounts of **12** and **13** produced from the chair structure of **4** were higher than that of **11** derived from boat intermediate **21** (the yield of **11** was only *ca.* 10% for all the enzymic products of the Trp mutants). Intermediate **4** could have undergone subsequent cyclization to give bicyclic **14** and **15**, but their amounts were relatively decreased with increasing amounts of monocyclic **12** and **13** when the bulkiness was increased (Table 3, compare L607W with L607F). Thus, the bulky Trp residue acted to interfere with the 2nd cyclization process (**4**→**5**).

It is noticeable that a slight difference in the steric bulk size at position 607 (compare Leu with Ile) had a remarkable influence on the substrate recognition (K_m), although the product distribution and the reaction velocity (k_{cat}) were almost the same as those of the wild-type (Tables 2 and 3). Substitution with the larger bulk size of Phe or Trp gave rise to a boat structure during the cyclization process. These findings seem to be informative in answering the question of why regio- and stereochemical control was attained for the polycyclization reaction. The exact steric bulk size of some or numerous active site residues may possibly guide the single stereoisomer, despite numerous isomers being possible. It has recently been shown that the mutation of Ile into Leu in cycloartenol synthase resulted in the production of lanosterol and parkeol besides cycloartenol, in spite of a little difference in the bulk size.[14] This report also validates the importance of the correct bulk size for directing the structural diversity of natural triterpenes.

In conclusion, this is the first report of a boat structure being constructed during the cyclization process by altering the enzyme structure, despite SHC always adopting an all *pre*-chair conformation for the construction of **2** and **3**. The introduction of a different steric bulk size at a given position(s) as the protocol for site-directed mutagenesis will be promising in future for creating unnatural natural products.

Acknowledgments

References

1) Hoshino, T., Insight into the active sites of squalene cyclase and the cyclization mechanism (in Japanese). *Bioscience & Industry*, **59**, 167–170 (2001).

2) Hoshino, T., and Sato, T., Squalene-hopene cyclase: catalytic mechanism and substrate recognition. *J. Chem. Soc. Chem. Commun.*, 291–301 (2002).

3) Abe, I., Rohmer, M., and Prestwich, G. D., Enzymatic cyclization of squalene and oxidosqualene to sterols and triterpenes. *Chem. Rev.*, **93**, 2189–2206 (1993).

4) Wendt, K. U., Schulz, G. E., Corey, E. J., and Liu, D. R., Enzyme mechanisms for polycyclic triterpene formation. *Angew. Chem. Int. Ed.*, **39**, 2812–2833 (2000).

5) Sato, T., and Hoshino, T., Functional analysis of the DXDDTA motif in squalene-hopene cyclase by site-directed mutagenesis experiments: initiation site of the polycyclization reaction and stabilization site of the carbocation intermediate of the initially cyclized A-ring. *Biosci. Biotechnol. Biochem.*, **63**, 2189–2198 (1999).

6) Hoshino, T., and Sato, T., Functional analysis of phenylalanine 365 in hopene synthase, a conserved amino acid in the families of squalene and oxidosqualene cyclases. *J. Chem. Soc. Chem. Commun.*, 2005–2006 (1999).

7) Hoshino, T., Kouda, M., Abe, T., and Ohashi, S., New cyclization mechanism for squalene: a ring expansion step for the five-membered C-ring intermediate in hopene biosynthesis. *Biosci. Biotechnol.*

Biochem., **63**, 2038–2041 (1999).

8) Sato, T., Abe, T., and Hoshino, T., On the cyclization mechanism of squalene: a ring expansion process of the five-membered D-ring intermediate. *J. Chem. Soc. Chem. Commun.*, 2617–2618 (1998).

9) Hoshino, T., Abe, T., and Kouda, M., Unnatural natural triterpenes produced by altering isoleucine into alanine at position 261 in hopene synthase and the importance of having the appropriate bulk size at this position for directing the stereochemical destiny during the polycyclization cascade. *J. Chem. Soc. Chem. Commun.*, 441–442 (2000).

10) Hoshino, T., Kouda, M., Abe, T., and Sato, T., Functional analysis of Phe605, a conserved aromatic amino acid in squalene-hopene cyclase. *J. Chem. Soc. Chem. Commun.*, 1485–1486 (2000).

11) Sato, T., and Hoshino, T., Catalytic function of the residues of phenylalanine and tyrosine conserved in squalene-hopene cyclases. *Biosci. Biotechnol. Biochem.*, **65**, 2233–2242 (2001).

12) Hart, E. A., Hua, L., Darr, L. B., Wilson, W. K., Pang, J., and Matsuda, S. P. T. Directed evolution to investigate steric control of enzymatic oxidosqualene cyclization. An isoleucine-to-valine mutation in cycloartenol synthase allows lanosterol and parkeol biosynthesis. *J. Am. Chem. Soc.*, **122**, 9887–9888 (1999).

13) Joubert, B. M., Hua, L., and Matsuda, S. P. T., Steric bulk at position 454 in *Saccharomyces cerevisiae* lanosterol synthase influences B-ring formation but not deprotonation. *Org. Lett.*, **2**, 339–341 (2000).

14) Matsuda, S. P. T., Darr, L. B. Hart, E. A., Herrera, J. B. R., McCann, K. E., Meyer, M. M., Pang, J., and Schepmann, H. G., Steric bulk at cycloartenol synthase. Position 481 influences cyclization and deprotonation. *Org. Lett.*, **2**, 2261–2263 (2000).

15) Tippelt, A., Jahnke, L., and Poralla, K., Squalene-hopene cyclase from *Methylococcus capsulatus* (Bath): a bacterium producing hopanoids and steroids. *Biochim. Biophys. Acta*, **1391**, 223–232 (1998).

16) Wendt, K. U., Poralla, K., and Schulz, G. E., Structure and function of a squalene cyclase. *Science*, **277**, 1811–1815 (1997).

17) Wendt, K. U., Lenhart, A., and Schulz, G. E., The structure of the membrane protein squalene-hopene cyclase at 2.0 Å resolution. *J. Mol. Biol.*, **286**, 175–187 (1999).

18) Merkofer, T., Pale-Grosdemange, C., Wendt, K. U., Rohmer, M., and Poralla, K., Altered product patterns of a squalene-hopene cyclase by mutagenesis of active site residues. *Tetrahedron Lett.*, **40**, 2121–2124 (1999).

19) Pale-Grosdemange, C., Merkofer, T., Rohmer, M., and Poralla, K., Production of bicyclic and tricyclic triterpenes by mutated squalene-hopene cyclase. *Tetrahedron Lett.*, **40**, 6009–6012 (1999).

20) Schmitz, S., Füll, C., Glaser, T., Albert, K., and Poralla, K., Specific production of γ-polypodatetraene or 17-isodammara-20(21), 24-diene by squalene-hopene cyclase mutant. *Tetrahedron Lett.*, **42**, 883–885 (2001).

21) Arai, Y., Hirohara, M., Ageta, H., and Hsü, H. Y., Fern constituents: two new triterpenoid alcohols with mono- and bi-cyclic skeletons, isolated from *Polypodiodes formosana. Tetrahedron Lett.*, **33**, 1325–1328 (1992).

22) Shiojima, K., Arai, Y., Masuda, K., Kamada, T., and Ageta, H., Fern constituents: polypodatetraenes, novel bicyclic triterpenoids, isolated from *Polypodiaceous* and *Aspidiaceous plants. Tetrahedron Lett.*, **24**, 5733–5736 (1983).

23) Douka, E., Koukko, A.-I., Drainas, C., Grosdemange-Billiard, C., and Rohmer, M., Structural diversity of the triterpenic hydrocarbons from the bacterium *Zymomonas mobilis*: the signature of defective squalene cyclization by the squalene/hopene cyclase. *FEMS Microbiol. Lett.*, **199**, 247–251 (2001).

24) Takeda, R., Naoki, H., Iwashita, T., Mizukawa, K., Hirose, Y., Ishida, T., and Inoue, M., Sesquiterpenoid constituents of the liverwort, *Ptychanthus striatus* (Lehm. et Lindenb. Nees). *Bull. Chem. Soc. Jpn.*, **56**, 1125–1132 (1983).

25) Nakamura, H., Wu, H., Kobayashi, J., Kobayashi, M., Ohizumi, Y., and Hirata, Y., Agelasidines. Novel hypotaurocyamine derivatives from the Okinawan sea sponge Agelas nakamurai Hoshino. *J. Org. Chem.*, **50**, 2494–2497 (1985).

26) Hoshino, T., and Sakai, Y., Enzymic products of the 2,3-oxidosqualene analog having an ethyl residue at 10-position. First trapping of the trimethylcyclohexanone ring by lanosterol synthase. *Tetrahedron Lett.*, **42**, 7319–7323 (2001).